

# Mitigating Thermal Gradients in Electric vehicle Battery Packs Using Star-Shaped Flow Deflectors

*Jose E. Cu-Rangel<sup>1</sup>, Carlos E. Oliva-Hernandez<sup>1</sup>, Miguel S. Núñez-Aguayo<sup>1</sup>  
J. Luis Luviano-Ortiz<sup>1</sup>, Abel Hernandez-Guerrero<sup>1,\*</sup>*

<sup>1</sup>University of Guanajuato, Department of Mechanical Engineering, Salamanca, Guanajuato, Mexico

\* Corresponding author

[je.curangel@ugto.mx](mailto:je.curangel@ugto.mx), [ce.olivahernandez@ugto.mx](mailto:ce.olivahernandez@ugto.mx), [ms.nunezaguayo@ugto.mx](mailto:ms.nunezaguayo@ugto.mx), [luis.luviano@ugto.mx](mailto:luis.luviano@ugto.mx),  
[abel@ugto.mx](mailto:abel@ugto.mx)

## Abstract

This study employs computational fluid dynamics (CFD) to evaluate the implementation of strategically placed star baffles within cylindrical battery packs in an electric vehicle. This geometric configuration is integrated to improve coolant flow dynamics and enhance heat transfer mechanisms throughout the system. Since non-uniform thermal gradients and excessive heat generation are the main drivers of accelerated cell degradation, controlling thermal distribution is critical to ensuring both energy efficiency and operational longevity. Integrating these star baffles effectively redirects coolant flow paths, mitigating stagnation zones and facilitating a more homogeneous thermal profile across the entire battery pack. Implementing the star baffles increased the maximum coolant velocity mitigating the formation of detrimental vortices within the battery pack. Comparative analysis with the reference geometry showed a reduction in peak temperature (from 327.16 K to 323.11 K), alongside a 3.1% decrease (10.3 K) in the most critical downstream zone. These parameters demonstrate an improved balance between thermal management efficiency and operational performance.

Keywords: Computational Fluid Dynamics; Star-Shaped Deflectors; Cylindrical Battery Packs; Electric Vehicles.

## 1 Introduction

Over the past several decades, the global community has faced an unprecedented environmental crisis. Anthropogenic pollution and accelerated climate change have solidified as the most critical, multifaceted challenges of the 21st century (Jochem et al., 2016). This ecological deterioration stems from the complex interplay of human activities, including intensive industrial manufacturing, large-scale power generation, rapid urban expansion and the ever-growing demands of the transportation sector. In this context, Internal Combustion Engine Vehicles (ICEVs) have been identified as a primary source of greenhouse gas emissions and air quality degradation due to their release of nitrogen oxides and particulate matter, especially in high-density urban areas. This profound impact on global energy balances and public health has catalyzed a global search for a radical technological shift toward sustainable mobility and carbon neutrality (Morgunov, 2024).

Electric Vehicles (EVs) have emerged as the leading technological solution to environmental concerns, representing a disruptive paradigm in modern transportation (Huluka et al., 2022). Beyond their ecological promise, EVs offer tangible benefits, such as eliminating acoustic pollution typical of ICEVs, significantly reducing mechanical ignition complexity, and improving energy utilization rates. From an economic perspective, EVs have lower operating and maintenance costs than fossil-fuel alternatives and ensure the complete absence of local tailpipe pollutants, a critical factor for the future of "green" smart cities (Calvin et al., 2019). Given these advantages, international market projections estimate that more than 125 million EVs will be in operation worldwide by 2030 as part of a coordinated global effort to curb vehicular emissions and reduce dependency on petroleum (Miao et al., 2019).

Lithium-ion (Li-ion) batteries are at the core of this transition. They have become the gold standard for energy storage due to their high specific energy, impressive power-to-weight ratios, and long-term operational efficiency (Tarascon et al., 2016; Sudworth et al., 2014). However, the mass-market scalability of these systems is hindered by significant technical challenges. High production costs are a critical barrier, largely due to the need for sophisticated Battery Management Systems (BMS) that require precise control and real-time monitoring of electrochemical variables (Atwell, 2019). Furthermore, as the industry pushes for higher energy densities and ultra-fast charging capabilities, internal heat generation within battery cells become increasingly pronounced. If not managed with high precision, this thermal energy leads to sharp thermal gradients and localized “hot spots” that can irreversibly degrade electrochemical performance, accelerate electrolyte aging, and ultimately threaten the structural safety of the entire battery pack by increasing the risk of thermal runaway.

To ensure the battery operates safely, reliably, and durably, its temperature must be strictly maintained within a narrow, stable window (typically between 15 °C to 35 °C) while achieving the most uniform thermal distribution possible across the entire pack (Ding et al., 2023). Conventional cooling channel or manifold designs, though widely used, often suffer from inherent fluid-dynamic limitations. These limitations include stagnation zones, preferential flow paths (channeling), and uneven heat transfer rates between the first and last cells in the series. These inefficiencies result in localized thermal peaks, creating imbalances in the State of Health (SoH) of the individual cells, compromising the system’s longevity (Rok et al., 2023).

In response to these limitations, the strategic integration of internal baffles into the cooling architecture has emerged as a promising, highly efficient strategy for refining fluid distribution. From a fluid mechanics perspective, baffles disrupt the boundary layer and redirect the flow into areas that would otherwise remain undercooled. This promotes turbulence and enhances the convective heat transfer coefficient. This approach significantly improves thermal homogeneity without requiring complex active cooling components or excessive increases in pumping power requirements. Consequently, this study proposes a detailed investigation into the inclusion of internal baffles within a fluid-cooled battery assembly (Vaz et al., 2025). The research focuses on analyzing the complex relationship between deflector geometry, flow distribution, and the resulting thermal behavior. The effectiveness of these elements in mitigating maximum temperatures and improving thermal uniformity was evaluated through a comparative analysis against a baseline configuration, thereby providing a pathway toward more robust and efficient battery thermal management systems. Figure 1 shows the base model of the battery train used for this research. It consists of 12 Panasonic NCR18650B batteries and a single-input, single-output module with the same cross-section.

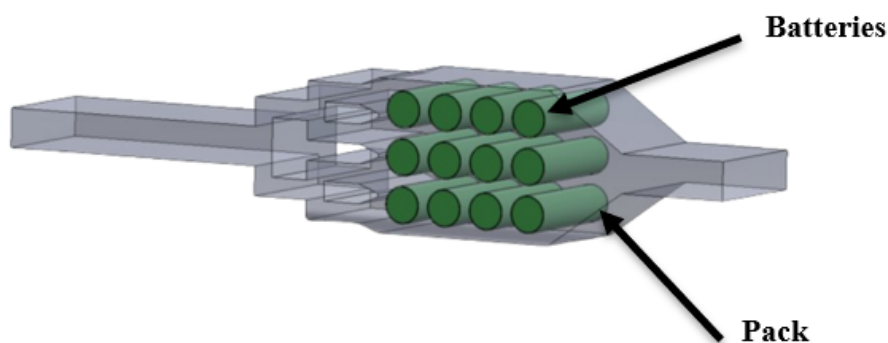


**Figure 1:** Base model.

## 2 Methodology

### 2.1 Model geometry

Two three-dimensional models of a lithium-ion battery pack were developed using computer-aided design (CAD) to analyze the case study. See Figure 2: a) Base Case, and b) Star Deflectors. Both models represent a module used in electric vehicles. To ensure consistent comparisons, both models

were designed under identical conditions; the only difference was the inclusion of star baffles in Case b). The star Deflectors are made of copper due to their high thermal conductivity, which enables these components to act as efficient heat spreaders that rapidly conduct thermal energy away from the cell surfaces. During the construction of the geometric model, the cells were strategically arranged within the module to promote a uniform distribution of airflow in the intercell spaces. This configuration allows for effective interaction between the coolant (air) and the batteries' external surfaces, thus facilitating convective heat transfer. Figure 2 shows the dimensions used for each case study.

The computational domain represents the cooling channel houses the cell array. It allows for fluid circulation and promotes the dissipation of heat generated during system operation. This setup aims to replicate the typical conditions of a Battery Thermal Management System (BTMS), where coolant is the primary medium to maintain operating temperatures within safe ranges and prevent the formation of steep thermal gradients or hot spots.

The system consists of an inlet section and an outlet section, both featuring rectangular geometry and located at opposite ends of the module. These straight extensions were incorporated to ensure the proper development of the flow velocity profile before the flow interacted with the cell array, as well as to mitigate potential numerical effects associated with boundary conditions within the simulation domain.

Furthermore, to improve flow distribution and mitigate the formation of thermal stagnation zones within the module, baffles were incorporated into the fluid domain. These elements were strategically positioned among the Li-ion battery cells to redirect the fluid toward regions with the highest temperature gradients. The geometry of the baffles was meticulously designed to promote flow redistribution and improve heat transfer without introducing excessive pressure drops or significant obstructions within the cooling channel.

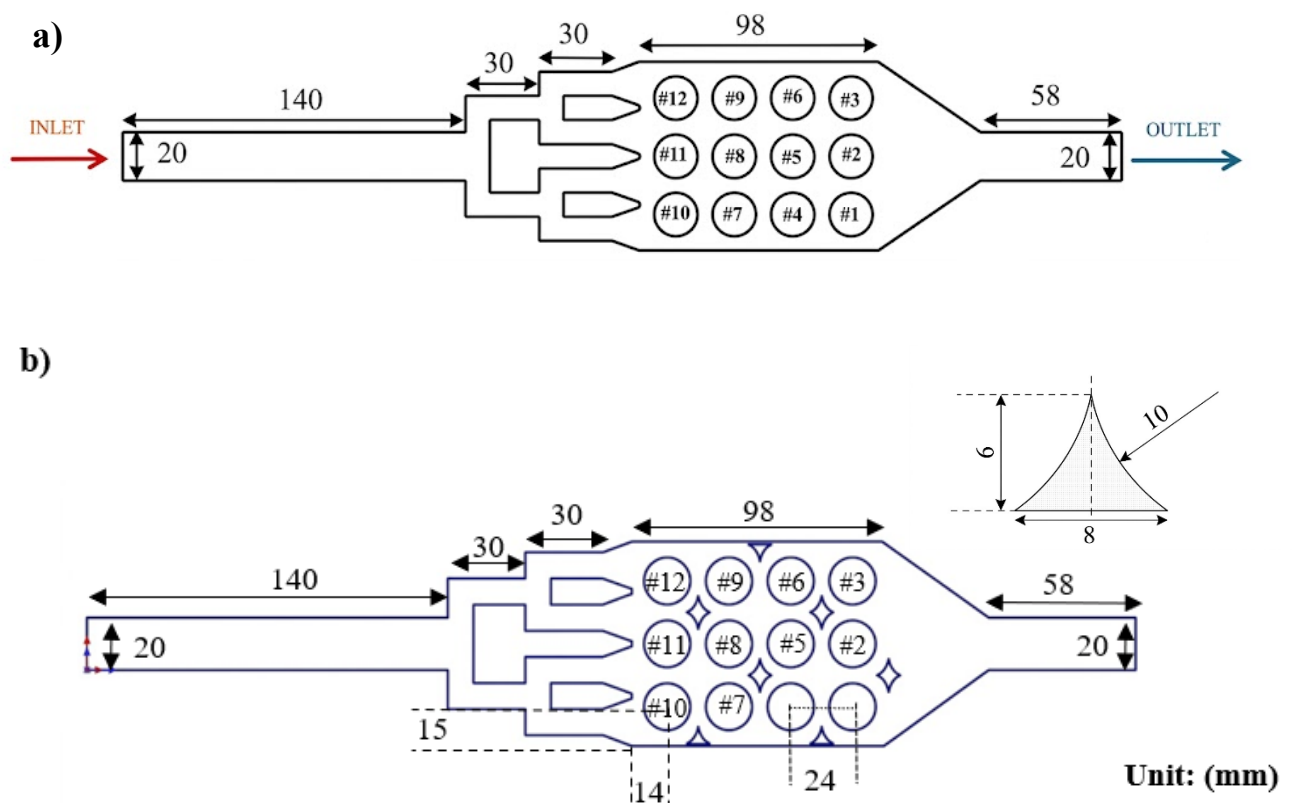


Figure 2: Dimensions for a) Base Case, and b) Star Deflectors Case.

## 2.2 Assumptions

To ensure numerical convergence and the physical representativeness of the thermal management system, the following assumptions were made:

1. **Steady-State Condition:** Flow and temperature variables are assumed to exhibit no significant temporal variations once the operational equilibrium is reached.
2. **Incompressible and Viscous Fluid:** Due to the low flow velocities (low Mach number), air is modeled as an incompressible fluid with constant viscous properties.
3. **Single-Phase Regime:** The coolant remains in the gaseous phase throughout the entire domain, neglecting any phase-change or condensation phenomena.
4. **Uniform Heat Generation:** A constant volumetric heat generation rate is assumed to be uniformly distributed within each cell, simplifying the thermal source associated with internal resistance.
5. **Negligible Radiation:** Since operating temperatures remain within moderate ranges of 15 °C to 35 °C, heat transfer by radiation is considered negligible compared to conduction and convection mechanisms.
6. **Constant Thermophysical Properties:** The properties of air and the battery materials are assumed to remain constant within the analyzed temperature range.

## 2.3 Governing equations

The thermo-fluid behavior of the battery pack cooling system was modeled by solving the governing equations of mass, momentum, and energy conservation for the airflow. Additionally, a resistance-based electrothermal model was used to describe heat generation within the cells.

In addition to the previously stated assumptions, the governing equations are solved using a Reynolds-averaged formulation. This formulation incorporates turbulence effects through an eddy-viscosity approach. Due to the relatively low flow velocities involved, the contribution of viscous dissipation to the energy equation is assumed to be negligible. Additionally, heat generation is assumed to occur exclusively within the solid domain (i.e., the battery cells), and there are no internal heat sources in the fluid region. Furthermore, the electrothermal model represents heat generation within the cells and applies it as a boundary condition at the solid–fluid interface to ensure consistency with the governing energy equations.

### Mass Conservation

Equation (1) represents the conservation of mass for an incompressible flow and is expressed through the continuity equation (where  $\vec{V}$  is the fluid velocity vector):

$$\nabla \cdot \mathbf{V} = 0 \quad (1)$$

### Momentum Conservation

The momentum equation for the fluid is given by:

$$\rho (\mathbf{V} \cdot \nabla) \mathbf{V} = -\nabla P + \nabla \cdot [(\mu + \mu_t) \nabla \mathbf{V}] \quad (2)$$

### Energy Conservation

The energy equations for the fluid and solid domains are given by:

$$\rho C_p (\mathbf{V} \cdot \nabla T_f) = k \nabla^2 T_f \quad (3)$$

$$\nabla \cdot (k_s \nabla T_s) + \dot{q} = 0 \tag{4}$$

This model allows for the representation of the non-uniform current distribution within the battery pack, which directly influences heat generation and the resulting temperature distribution of the system.

### Turbulence Model

The  $k - \varepsilon$  turbulence model is described by the following equations:

$$\rho(\mathbf{V} \cdot \nabla k) = \nabla \cdot \left( \frac{\mu_t}{\sigma_k} \nabla k \right) + P_k - \rho \varepsilon \tag{5}$$

$$\rho(\mathbf{V} \cdot \nabla \varepsilon) = \nabla \cdot \left( \frac{\mu_t}{\sigma_\varepsilon} \nabla \varepsilon \right) + C_{1\varepsilon} \frac{\varepsilon}{k} P_k - C_{2\varepsilon} \rho \frac{\varepsilon^2}{k} \tag{6}$$

## 2.4 Boundary conditions

Table 1 presents the operating conditions and material properties used in this study. To ensure a consistent comparison between different configurations and to assess cell performance, the evaluated cases were analyzed under identical parameters. An inlet velocity of 3 m/s and an operating temperature of 300 K were set. Figure 3 shows the thermophysical properties of the materials that were considered for this case study.

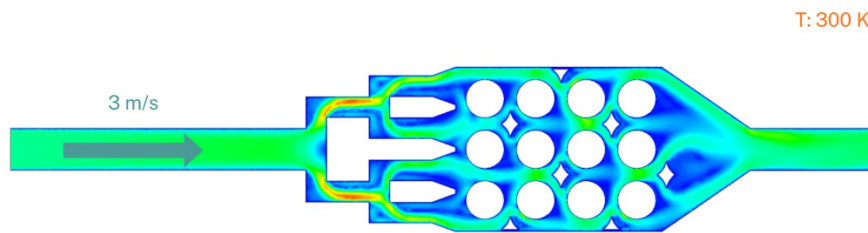


Figure 3: Conditions of the Case Study.

Table 1. Thermophysical properties of materials.

Material	$\rho$ [kg/m <sup>3</sup> ]	$C_p$ [J/kg·K]	$k$ [W/m·K]	$\mu$ [kg/m·s]
Air	1.225	1006	0.0242	$1.81 \times 10^{-5}$
Battery	2018	1282	2.7	–
Copper	8960	385	401	–

## 2.5 Numerical model

The thermal and fluid-dynamic analysis of the battery pack was performed using Computational Fluid Dynamics (CFD), employing a numerical approach capable of describing the transport phenomena of mass, momentum, and energy that governs air cooling. This approach enables a detailed evaluation of the flow distribution and temperature gradients within the computational domain, providing an accurate description of the system’s thermal performance.

The governing equations—including those for the conservation of mass, Navier–Stokes, and energy—were discretized using the finite volume method, ensuring both local and global conservation of the physical quantities. Turbulence effects were modeled using the realizable  $k - \varepsilon$  model, which provides improved accuracy for flows involving strong streamline curvature and recirculation. The pressure–

velocity coupling was solved using the SIMPLE algorithm, which employs an iterative correction procedure to ensure compliance with the continuity equation. Combining these methods with the finite volume scheme provides a robust and stable numerical solution, suitable for simulating complex internal flows in battery pack cooling systems.

## 2.6 Validation/mesh independence

### 2.7.1 Validation

To validate the developed numerical model, a comparison was carried out with experimental data reported by Xie et al. (2021), where the thermal behavior of a lithium-ion battery pack was evaluated under controlled conditions. Experiments were conducted at a discharge rate of 1C, with a constant current, a state of charge (SOC) of 0.4, and an ambient temperature of 27 °C.

Unlike the transient model presented in the reference study, it is important to note that the model implemented in this work assumes steady-state conditions. However, Xie indicates that the electro-thermal model can be adapted to different operating conditions, thus supporting the validity of this approach.

Validation was performed by comparing the average surface temperature of each battery cell and evaluating the relative error between the numerical predictions and the experimental data. Figure 4 shows the average relative error obtained for each of the 12 cells in the battery pack.

The results indicate that the relative error remains below 1% for all cells, ranging from approximately 0.03% to 0.88%. The highest deviations were observed in cells 3 and 6, while the lowest errors correspond to cells 8 and 12. Despite these variations, all values remain within a very low error range, demonstrating the high accuracy of the model.

Overall, these results demonstrate excellent agreement between the simulation and experimental data. This validates the model's ability to accurately predict the system's thermal behavior. Furthermore, the results confirm that the steady-state assumption adequately represents the phenomenon under the analyzed conditions.

Therefore, the proposed model is a reliable tool for thermal analysis and designing cooling systems for lithium-ion battery packs.

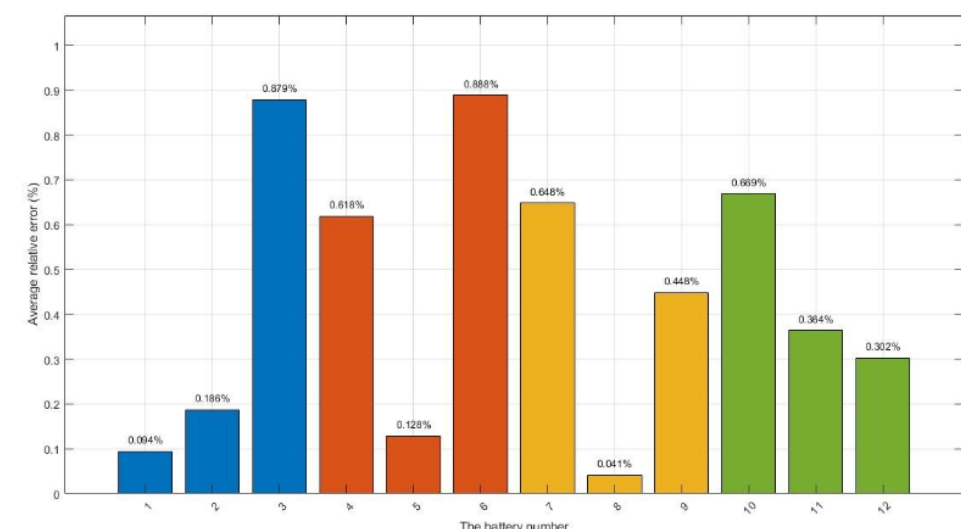


**Figure 4:** Average relative error per cell under 1C discharge at 27 °C.

### 2.7.2 Mesh independence

To ensure the results were not dependent on the mesh refinement level, a mesh convergence study was performed. Seven mesh configurations with an increasing number of elements were generated for this purpose.

Mesh independence was analyzed by evaluating the temperature variation of battery number 12 under identical conditions. The results showed that, with a mesh of approximately 1,500,000 elements, the variations became negligible, indicating that the numerical solution is independent of further mesh refinement. Figure 5 shows the behavior of the analyzed variable in relation to the number of mesh elements, clearly demonstrating the convergence of the solution.

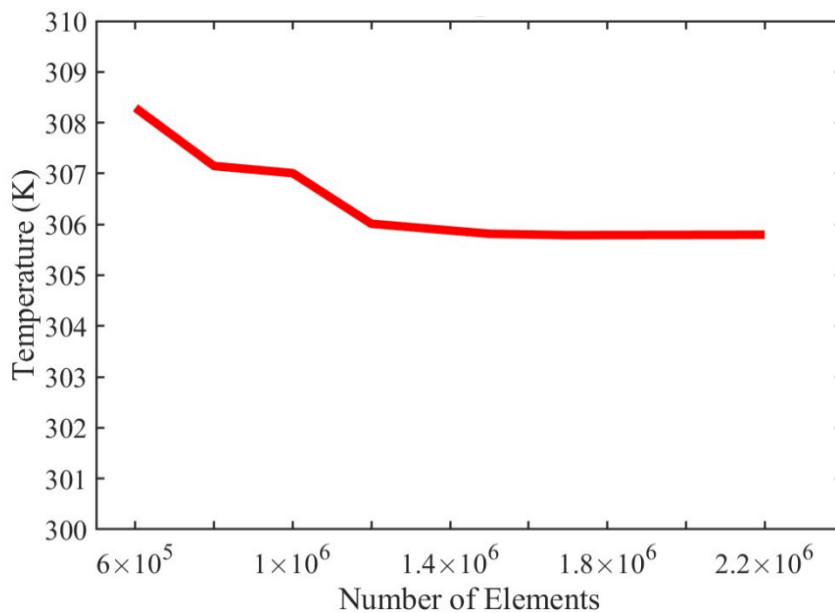


Figure 5: Mesh independence.

## 3 Results and discussion

The performance of each configuration was evaluated based on three key thermal management parameters: velocity distribution, temperature profiles across the module, and overall temperature distribution. Through a comparative analysis of these cases Sahin et al. (2022) demonstrate that strategically implementing copper baffles optimizes flow uniformity and mitigates thermal gradients, which are fundamental to safeguarding the operational integrity and efficiency of energy storage systems in electric vehicles.

### 3.1 Flow dynamics and velocity distribution

The addition of star-shaped baffles significantly altered the fluid dynamic behavior within the battery pack. As shown in the velocity contours in Figure 6, the reference configuration, Case a), exhibits preferential flow paths, where the coolant surrounds the central cells of the battery, potentially creating stagnation zones. These stagnation zones are associated with the formation of relatively large and stable recirculation vortices in the rear and between the cells, resulting from boundary layer separation as the flow interacts with the cylindrical geometries. These vortices limit fluid renewal and reinforce the presence of low-velocity areas, especially in the central region of the array.

Introducing the deflectors, Case b), increased the maximum flow velocity slightly, from 6.88 m/s to 7.22 m/s an increase of approximately 4.94%. More importantly, the baffles disrupted the boundary layer and redirected the airflow toward the central region of the array. This promotes more homogeneous flow interaction with the cell surfaces, effectively mitigating stagnant zones. Additionally, the baffles

modify the vortical flow structure by breaking up large vortices into smaller, more distributed ones and generating secondary vortices at their edges. This increases fluid mixing and reduces the persistence of stagnant recirculation, resulting in better refrigerant distribution.

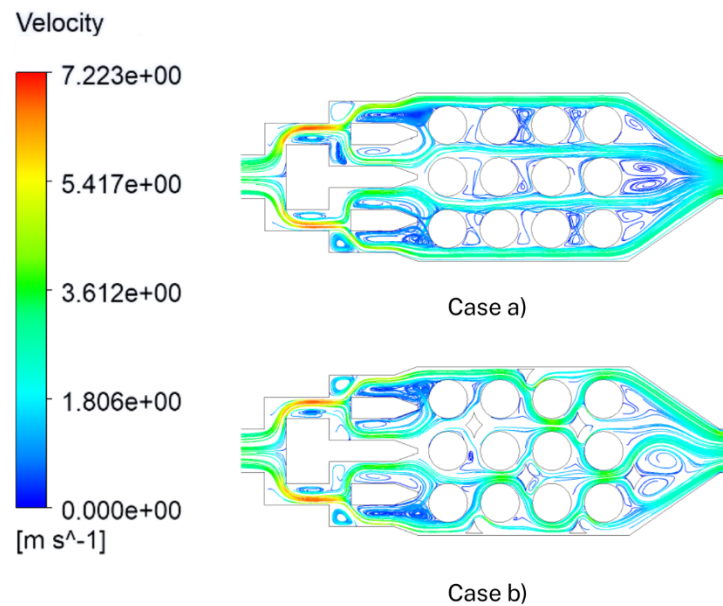


**Figure 6:** Velocity field distribution for Cases a) and b).

## 3.2 Thermal distribution and heat mitigation

The primary objective of the proposed thermal management system is to maintain a uniform temperature profile and prevent localized hot spots. Figure 7 shows that the temperature contours demonstrate a clear improvement in cooling capacity when the star-shaped deflectors are utilized. In the baseline model without deflectors, the maximum temperature was 328.2 K, with heat accumulating predominantly in the downstream region of the battery module due to insufficient coolant flow. In contrast, implementing the copper star deflectors reduced the maximum temperature to 319.6 K, a reduction of approximately 8.6 K, which is highly significant for ensuring the operational longevity of lithium-ion batteries. The copper deflector's high thermal conductivity enabled them to act as efficient heat spreaders. Combined with the improved convective heat transfer from the redirected airflow, this facilitated faster thermal dissipation and a much more uniform temperature profile across the entire pack.

### 3.2.1 Thermal distribution and comparative analysis of individual cell behavior

Figure 8 presents the detailed thermal behavior of each cell in the battery pack and compares the performance of the twelve cells, divided into two control groups. It illustrates the maximum temperatures reached in the base configuration, Case a), and the proposed design with star-shaped deflectors, Case b). To obtain a better visualization of the results, 315 K was set as the maximum temperature within the Figure; however, the actual temperatures were reported below.

Under the conditions of Case a), a tendency toward progressive heating is observed as the fluid moves through the array, cells 6 and 9 are identified as the point of greatest thermal stress at 328.2 K. Without redirection elements, the airflow does not effectively penetrate the central cavities of the pack, generating stagnant zones that compromise the integrity of the subsequent cells.

In Case b), incorporating copper baffles modifies the system's fluid dynamics, significantly improving thermal performance. The implementation of these geometries substantially reduces the temperature of cell 6 to 311.6 K, and similarly, cell 9 reduced its temperature to 319.6 K. This decrease observed in the batteries is clear evidence that the baffles induce alterations in the boundary layer, thus favoring an increase in the convective heat transfer coefficient.

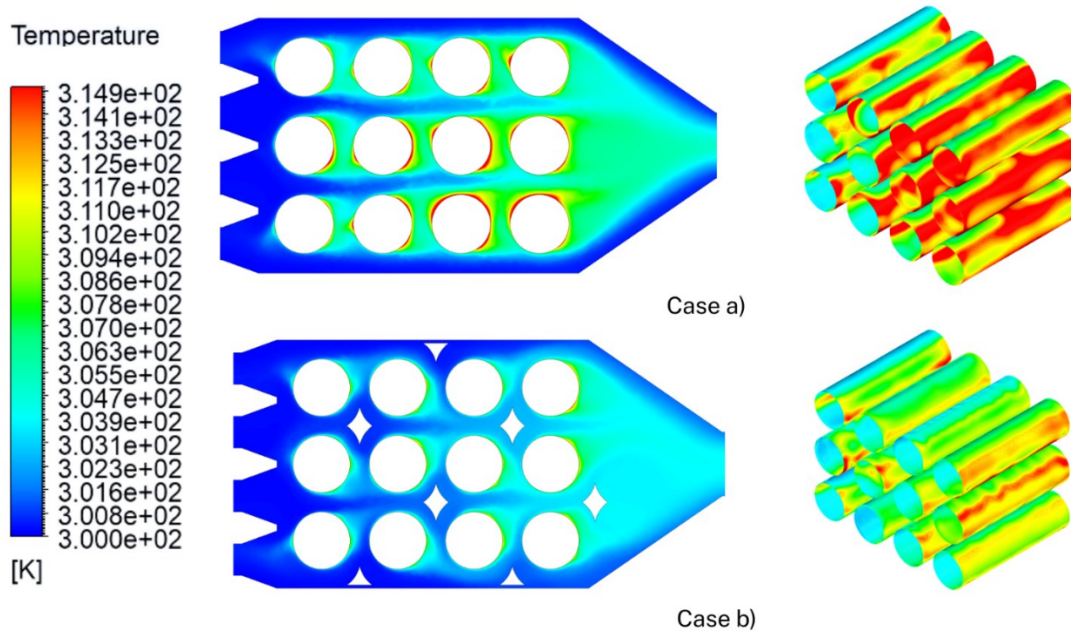


**Figure 7:** Comparison of temperature distribution in Case a) and b).

Furthermore, the comparison reveals that Case b) exhibits much smaller thermal deviation between adjacent cells than Case a). While the base model shows differences of up to 8.29 K between neighboring cells, the baffle-equipped model maintains a much more balanced profile, reducing thermal deviations by approximately 60–70%. This homogenization is essential for the operation of electric vehicles because it prevents disparities in internal resistance caused by heat, thus ensuring a longer lifespan and operational stability of the energy storage system.

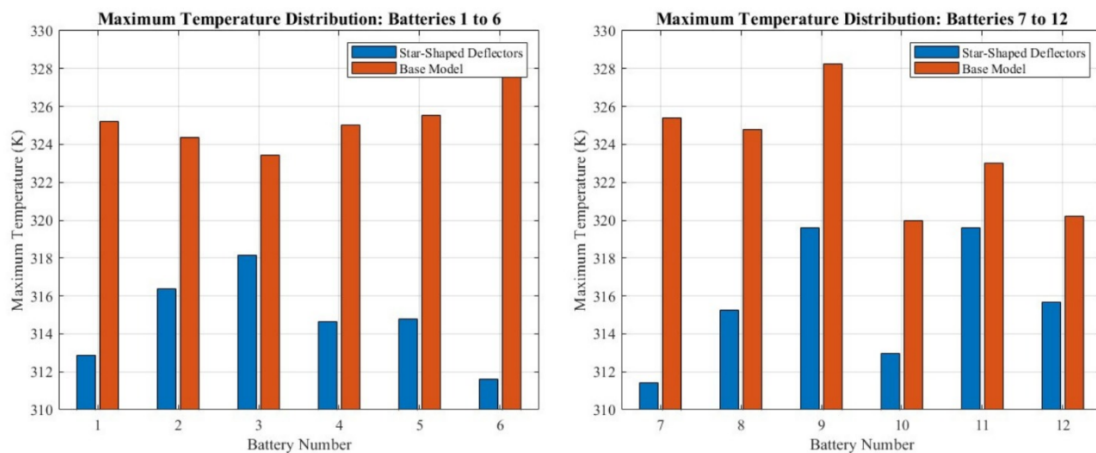


**Figure 8:** Maximum temperatures per cell: a) Base Configuration and b) Star Deflectors Configuration.

## 4 Conclusions

- This study evaluated the impact of incorporating star-shaped baffles on the thermo-fluid dynamic behavior of a lithium-ion battery pack for electric vehicles. By comparing a baseline configuration with a modified one, substantial improvements in flow distribution and thermal management of the system were identified. The model was validated using experimental data reported in the literature, yielding errors of less than 1%, which supports the accuracy and reliability of the methodology employed. The results demonstrate the effectiveness of the baffles in redistributing airflow and promoting thermal uniformity.
- A three-dimensional numerical model was developed under steady-state conditions to allow for a detailed analysis of the interaction between airflow and heat generation within the cells. This model provides a practical framework for assessing the influence of internal flow deflectors on thermal behavior and airflow patterns, enabling designers to understand their impact without assuming optimal performance.
- The inclusion of copper baffles significantly altered the flow distribution by eliminating preferential paths and reducing stagnation zone formation within the module. From a fluid dynamics perspective, the vortex structure transformed from large, stable vortices in the baseline case to smaller, more distributed structures, thereby increasing fluid mixing and enhancing convective heat transfer. These changes highlight the role of internal geometries in passively improving flow behavior without adding active pumping requirements.
- The implementation of baffles decreased the system's maximum temperature by approximately 4 K. Additionally, thermal gradients between cells decreased in critical regions, allowing decrease of temperature of up to 10 K. This helps to mitigate the formation of hot spots.
- The high thermal conductivity of copper allows the baffles to act as passive heat sinks, promoting more uniform heat distribution throughout the battery pack. This passive strategy is a low-cost, low-complexity solution that can be easily applied to different battery pack designs and could complement active cooling systems.
- Overall, the results demonstrate that incorporating star-shaped baffles is an efficient, passive, and cost-effective approach to optimizing thermal management in battery packs. This work represents a valuable contribution by providing a clear design methodology and quantitative insight into passive flow control strategies for electric vehicle battery systems.

## NOMENCLATURE

$C_p$	Specific heat of the fluid	(J/kg · K)
$k$	Thermal conductivity	(W/m <sup>2</sup> · K)
$P$	Pressure	(Pa)
$T$	Temperature	(K)
$V$	Velocity Magnitude	(m/s)
$x, y, z$	Cartesian components	(m)

### Greek symbols

$\rho$	Density	(kg/m <sup>3</sup> )
$\mu$	Dynamic viscosity	(N · s/m <sup>2</sup> )

## REFERENCES

- Blomgren, G. E., "The Development and Future of Lithium Ion Batteries," *J. Electrochem. Soc.*, vol. 164, no. 1, p. A5019, 2017, doi: 10.1149/2.0251701jes.
- Jochem, P. et al., "Climate change and transport," *Transportation Research Part D: Transport and Environment*, vol. 45, pp. 1–3, 2016, doi: 10.1016/j.trd.2016.03.001.
- Huluka, A. et al., "Numerical Study on the Design of Air Cooled Battery Thermal Management System for Eco-friendly Vehicles," *Int. J. Automotive Technol.*, vol. 23, pp. 603–612, Jun. 2022, doi: 10.1007/s12239-022-0054-2.
- Kim, J. et al., "Numerical study on thermal characteristics of an air-cooled lithium-ion battery pack with different flow configurations," *International Journal of Automotive Technology*, vol. 23, no. 3, pp. 819–829, 2022, doi: 10.1007/s12239-022-0055-5.
- Miao, Y. et al., "Current Li-Ion Battery Technologies in Electric Vehicles and Opportunities for Advancements," *Energies*, vol. 12, no. 6, Art. no. 1074, Mar. 2019, doi: 10.3390/en12061074.
- Morgunov, B. et al., "Health Risk Factors of Emissions from Internal Combustion Engine Vehicles: An Up-to-Date Status of the Problem," *Health Risk Analysis*, 2024, doi: 10.21668/health.risk/2024.1.18.eng.
- Sahin, R. et al., "Thermal management system for air-cooled battery packs with flow-disturbing structures," *J. Power Sources*, vol. 551, p. 232214, Dec. 2022, doi: 10.1016/j.jpowsour.2022.232214.
- Sudworth, J. L., "The sodium/nickel chloride (ZEBRA) battery," *J. Power Sources*, vol. 100, nos. 1–2, pp. 149–163, Nov. 2001, doi: 10.1016/S0378-7753(01)00891-6.
- Tarascon, J. M., "The Li-Ion Battery: 25 Years of Exciting and Enriching Experiences," *Electrochem. Soc. Interface*, vol. 25, no. 1, pp. 79–87, 2016.
- Tie, S., "A review of energy sources and energy management system in electric vehicles," *Renew. Sustain. Energy Rev.*, vol. 20, pp. 82–102, apr. 2013, doi: 10.1016/j.rser.2012.11.077.
- Vaz, F. et al., "CFD-Driven Design of an Air-Cooling System for Lithium-Ion Battery Packs in a Formula Student Car," *Energies*, vol. 18, no. 20, p. 5436, Oct. 2025, doi: 10.3390/en18205436.
- Xi, Y. et al., "A resistance-based electro-thermal coupled model for an air-cooled battery pack that considers branch current variation," *International Journal of Thermal Sciences*, vol. 159, p. 106611, 2021, doi: 10.1016/j.ijthermalsci.2020.106611.
- Arcus, C., "Exciting Developments in NMC 811 Lithium Battery Technology," *CleanTechnica*, 2018. [Online]. Available: <https://cleantechnica.com/>. [Accessed: Mar. 10, 2026].
- "Six Li-ion Battery Chemistries: Not All Batteries Are Created Equal," *Power Electronics*. [Online]. Available: <https://www.powerelectronics.com/alternative-energy/six-Li-ion-battery-chemistries-not-all-batteries-are-created-equal>. [Accessed: Mar. 10, 2026].
- Thomas, C., Objects to "Chauffeur". *The New York Times*. Available online: <https://timesmachine.nytimes.com/timesmachine/1902/01/22/101930350.pdf>